ISSN 2277-2685
IJESR/March. 2022/ Vol-12/Issue-1/1-14
A. Srinivasa Rao *et. al.,* / International Journal of Engineering & Science Research

Load Carring Analysis In The Finite Journal Bearing With Parameters Fluid Pressure, Thermal Factor and Viscosity

1. Mr.A.Srinivasa Rao[1], Asst.Professor, Rise Krishna Sai Prakasam Goup of Institutions, Ongle, A.P., India.

2. Dr.M. Ganapathi[2], Professor, Rise Krishna Sai Gandhi Goup of Institutions, Ongle, A.P., India.

Abstract: This research examines the impacts of additives on lubrication with viscosity change and temperature effects, published in the Finite Journal. For finite journal bearing, the generalized Reynolds equation for two-layer fluid is developed and applied. The Finite Difference Method approach is used to solve the finite journal bearing with modified Reynolds equation numerically. The pressure and load capacity in the lubrication process rise as the temperature impact for two-layer fluids grows.

Keywords: Viscosity, eccentricity, film thickness, thermal effect, and finite journal bearing.

1.1 INTRODUCTION:

In general, it can be said that the majority of lubricated systems are composed of moving (stationary) surfaces (plane, curve, or loaded/unloaded) separated by a thin film of an external substance (lubricant). Such a thin coating between these surfaces not only reduces friction but also aids in supporting heavy loads. The nature of the surfaces, the nature of the lubricant film boundary conditions, etc., determine the characteristics of the system, such as pressure in the film, frictional force at the surface, flow rate of lubricant, etc.

The "Reynolds Equation"which was initially developed by Reynolds is the equation that controls the pressure created in the lubricating layer and may be found by connecting the equation of motion with the equation of continuity. The influences of temperature, compressibility, viscosity fluctuation, slip at the surface, inertia, and surface roughness were disregarded in the development of this equation. Later, the viscosity and density variations along the fluid film are included to the Reynolds equation.

This research analyzes the lubrication of Finite journal bearings under operating conditions while taking into account the impacts of additives and heat factors. The issue with lubricant additives is solved using the generalized Reynolds' equation. Applying the finite difference approach to the pertinent equations allows for the derivation and numerical solution of the load capacity and pressure expressions. By taking into account changes in viscosity, thermal impacts are taken into account, and appropriate load capacity graphs are displayed to see their consequences.

1.2 Governing Equation:

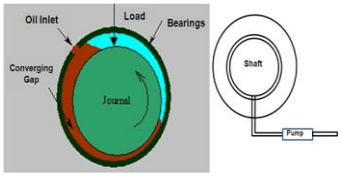

Fig 1.1: Finite Journal bearing configuration

The Physical configuration of the finite journal bearing in fig (1.1), C be the clearance of the bearing C =R-r, $\varepsilon = \frac{e}{c}$ be the eccentricity ratio and 'h' is the total film thickness, is given by $h = c(1+\varepsilon\cos\theta)$ are shown in fig (1.1).

$$\frac{\partial h}{\partial \theta} = -c\varepsilon\sin\theta \tag{1.1}$$

Reynold's equation, which governs the flow of fluid in the bearing, is presented.

$$\frac{\partial}{\partial x}\left[\frac{h^3}{12\mu}F\frac{\partial p}{\partial x}\right]+\frac{\partial}{\partial y}\left[\frac{h^3}{12\mu}F\frac{\partial p}{\partial y}\right]=U\frac{\partial h}{\partial x} \tag{1.2}$$

$$F=\frac{(1-\frac{a}{h})^3(k-1)+1}{k} \tag{1.3}$$

Considering thermal effect and viscosity, μ can be taken as $\mu=\mu_0(\frac{h}{h_0})^q$ (1.4)

Where q is thermal factor
Then the non-dimensional parameters are

$$x=R\theta,\ dx=Rd\theta,\ \bar{y}=\frac{y}{L}\Rightarrow y=\bar{y}L, dy=Ld\bar{y},\ \bar{\mu}=\frac{\mu_0}{h_0^q} \tag{1.5}$$

$$\frac{\partial}{R\partial\theta}\left[\frac{h^3}{12\mu_0(\frac{h}{h_0})^q}F\frac{\partial p}{R\partial\theta}\right]+\frac{\partial}{L\partial\bar{y}}\left[\frac{h^3}{12\mu_0(\frac{h}{h_0})^q}F\frac{\partial p}{L\partial\bar{y}}\right]=\frac{U}{R}\frac{\partial h}{\partial\theta} \tag{1.6}$$

$$\frac{\partial}{R\partial\theta}\left[\frac{h_0^q}{12\mu_0}h^{(3-q)}F\frac{\partial p}{R\partial\theta}\right]+\frac{\partial}{L\partial\bar{y}}\left[\frac{h_0^q}{12\mu_0}h^{(3-q)}F\frac{\partial p}{L\partial\bar{y}}\right]=\frac{U}{R}\frac{\partial h}{\partial\theta} \tag{1.7}$$

By substituting equation (1.5) in (1.7), then the modified Reynolds equation in a non-dimensional form can be written as

$$\frac{\partial}{R\partial\theta}\left[\frac{\bar{h}^{(3-q)}}{12\bar{\mu}}\bar{F}\frac{\partial p}{R\partial\theta}\right]+\frac{\partial}{L\partial\bar{y}}\left[\frac{\bar{h}^{(3-q)}}{12\bar{\mu}}\bar{F}\frac{\partial p}{L\partial\bar{y}}\right]=\frac{U}{R}\frac{\partial h}{\partial\theta} \tag{1.8}$$

$$\text{put } \lambda^2=\frac{L^2}{4R^2},\ \bar{F}=\frac{(1-\frac{\bar{a}}{\bar{h}})^3(k-1)+1}{k},\ \bar{h}=c(1+\varepsilon\cos\theta) \tag{1.9}$$

By solving the above equation (1.7), we get the non- dimensional pressure as

$$\bar{p}=\frac{pc^2}{\mu uR} \tag{1.10}$$

Now the equation (1.7) reduced to

$$\frac{\partial}{\partial\theta}\left[\bar{F}\bar{h}^{(3-q)}\frac{\partial\bar{p}}{\partial\theta}\right]+\frac{1}{4\lambda^2}\frac{\partial}{\partial\bar{y}}\left[\bar{F}\bar{h}^{(3-q)}\frac{\partial\bar{p}}{\partial\bar{y}}\right]=-12\varepsilon\sin\theta \tag{1.11}$$

The following are the boundary conditions for fluid film pressure

$$\begin{aligned}&\bar{p}=0\ at\ \ \theta=0\\&\bar{p}=0\ at\ \ \theta=\pi\end{aligned} \tag{1.12}$$

The finite difference approach is used to numerically solve the modified Reynolds equation. Grid points are used to partition the film domain under investigation, as seen in fig. (1.2). The terms of equation (1.11) can be represented as follows in finite increment format

$$\begin{aligned}&\frac{\bar{h}^{(3-q)}}{\Delta\theta}\left[\left[\bar{F}_{i+\frac{1}{2},j}\left(\frac{\bar{p}_{i,j}-\bar{p}_{i-1,j}}{\Delta\theta}\right)\right]-\left[\bar{F}_{i-\frac{1}{2},j}\left(\frac{\bar{p}_{i+1,j}-\bar{p}_{i,j}}{\Delta\theta}\right)\right]\right]+\\&\frac{\bar{h}^{(3-q)}}{4\lambda^2}\frac{1}{\Delta\bar{y}}\left[\bar{F}_{i,\,j+\frac{1}{2}}\left(\frac{\bar{p}_{i,j}-\bar{p}_{i,j-1}}{\Delta\bar{y}}\right)-\left[\bar{F}_{i,\,j-\frac{1}{2}}\left(\frac{\bar{p}_{i,j+1}-\bar{p}_{i,j}}{\Delta\bar{y}}\right)\right]\right]=-12\varepsilon\sin\theta\end{aligned} \tag{1.13}$$

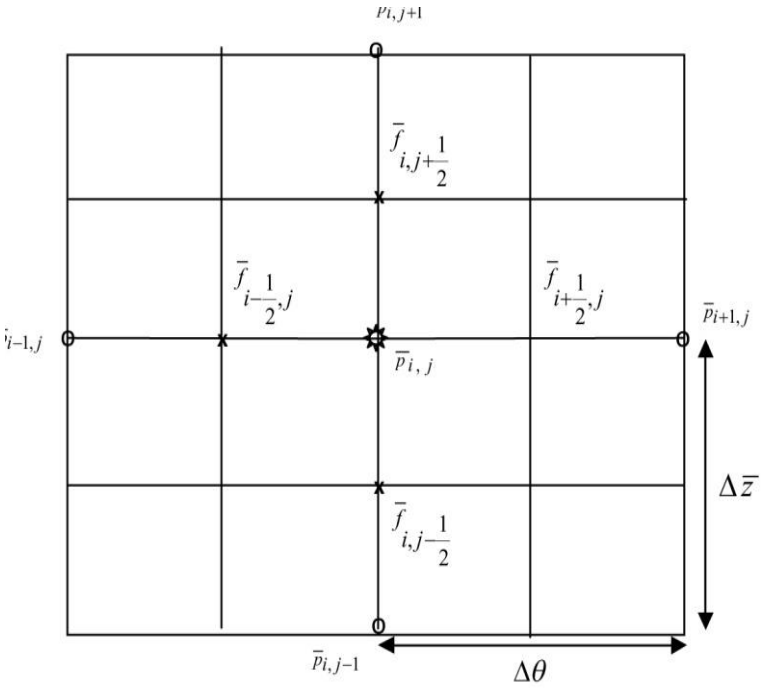

Fig 1.2: Grid point notation for film domain

By solving the equations

$$\frac{\bar{h}^{(3-q)}}{(\Delta\theta)^2}\left[\bar{F}_{i+\frac{1}{2},j}\bar{p}_{i,j}-\bar{F}_{i+\frac{1}{2},j}\bar{p}_{i-1,j}-\bar{F}_{i-\frac{1}{2},j}\bar{p}_{i+1,j}+\bar{F}_{i-\frac{1}{2},j}\bar{p}_{i,j}\right]+$$
$$\frac{\bar{h}^{(3-q)}}{4\lambda^2}\frac{1}{\Delta\bar{y}^{-2}}\left[\bar{F}_{i,j+\frac{1}{2}}\bar{p}_{i,j}-\bar{F}_{i,j+\frac{1}{2}}\bar{p}_{i,j-1}-\bar{F}_{i,j-\frac{1}{2}}\bar{p}_{i,j+1}+\bar{F}_{i,j-\frac{1}{2}}\bar{p}_{i,j}\right]=-12\varepsilon\sin\theta \quad (1.14)$$

By substituting this equation in (1.11), we have

$$\bar{p}_{i,j}\bar{h}^{(3-q)}\left[4\lambda^2r^2\left(\bar{F}_{i+\frac{1}{2},j}+\bar{F}_{i-\frac{1}{2},j}\right)+\left(\bar{F}_{i,j+\frac{1}{2}}+\bar{F}_{i,j-\frac{1}{2}}\right)\right]=-48\,\varepsilon\,\lambda^2\Delta\bar{y}^{-2}\sin\theta+\bar{h}^{(3-q)}[4\lambda^2r^2\bar{F}_{i+\frac{1}{2},j}\bar{p}_{i-1,j}$$
$$+4\lambda^2r^2\bar{F}_{i-\frac{1}{2},j}\bar{p}_{i+1,j}+\bar{F}_{i,j+\frac{1}{2}}\bar{p}_{i,j-1}+\bar{F}_{i,j-\frac{1}{2}}\bar{p}_{i,j+1}] \quad (3.15)$$

$$c_0\bar{p}_{i,j}\bar{h}^{(3-q)}=\bar{h}^{(3-q)}[4\lambda^2r^2\bar{F}_{i+\frac{1}{2},j}\bar{p}_{i-1,j}+4\lambda^2r^2\bar{F}_{i-\frac{1}{2},j}\bar{p}_{i+1,j}+\bar{F}_{i,j+\frac{1}{2}}\bar{p}_{i,j-1}+\bar{F}_{i,j-\frac{1}{2}}\bar{p}_{i,j+1}]$$
$$-48\,\varepsilon\,\lambda^2\Delta\bar{y}^{-2}\sin\theta \quad (1.16)$$

$$\bar{p}_{i,j} = c_1 \bar{p}_{i-1,j} + c_2 \bar{p}_{i+1,j} + c_3 \bar{p}_{i,j-1} + c_4 p_{i,j+1} + c_5 \qquad (1.17)$$

The coefficient c_0, c_1, c_2, c_3, c_4, c_5, defined as

$$c_0 = \left[4\lambda^2 r^2 \left(\bar{F}i+\frac{1}{2},j + \bar{F}i-\frac{1}{2},j \right) + \left(\bar{F}i,j+\frac{1}{2} + \bar{F}i,j-\frac{1}{2} \right) \right], c_1 = \frac{4\lambda^2 r^2 \bar{F}i+\frac{1}{2},j}{c_0}, c_2 = \frac{4\lambda^2 r^2 \bar{F}i-\frac{1}{2},j}{c_0}$$

$$, c_3 = \frac{\bar{F}i,j+\frac{1}{2}}{c_0}, c_4 = \frac{\bar{F}i,j-\frac{1}{2}}{c_0}, \text{and } c_5 = \frac{-48\lambda^2 \Delta \bar{y}^{-2} \varepsilon \sin\theta}{c_0 \bar{h}^{(3-q)}} \qquad (1.18)$$

$\bar{r} = \frac{\Delta \bar{z}}{\Delta \bar{\theta}}$ The pressure p is calculated numerically with grid spacing of $\Delta\bar{\theta} = 9°$ and $\Delta\bar{z} = 0.05$

As a result of the film pressure, the bearing W's load carrying capacity is calculated by

$$W = \int_{\theta=0}^{\theta=\pi} \int_{z=0}^{z=\frac{1}{2}} p \cos\theta \, d\theta dz \qquad (1.19)$$

By using (3.12)in (3.17), we get non dimensional load as

$$\bar{W} = \frac{WC^2}{\mu UR} = \int_{\theta=0}^{\theta=\pi} \int_{z=0}^{z=\frac{1}{2}} p \cos\theta \, d\bar{\theta} d\bar{z} \qquad (1.20)$$

$$\approx \bar{w} = \sum_{i=0}^{M} \sum_{j=0}^{N} \bar{p}_{ij} \Delta\bar{\theta} \, \Delta\bar{z} \qquad (1.21)$$

Where M+1 and N+1 are, respectively, the grid point numbers along the 'x' and 'z' axes.

The analysis, numerical solution, and graphing of the pressure and the dimensionless load capacity are performed.

1.3 RESULTS AND DISCUSSIONS:

The mesh of the film domain in equation (1.17) for pressure contains 20 equal intervals along the bearing length and circumference. The system of algebraic equations' coefficient matrix has a pentadiagonal shape. Sci-lab tools have been used to resolve these equations.

PRESSURE:

The variation of non-dimensional pressure ' $\bar{p}$ 'for different values of 'q' with $\bar{a}$ =0.1and R=1.5 is shown in fig (1.3). It is observed that ' $\bar{p}$ 'decreases for increasing value of 'q'.

Fig (1.4) shows the variation of film pressure '$\bar{p}$ and different values of peripheral layer thickness '$\bar{a}$', with k=0.5 and R=1.5.It is observed that '$\bar{p}$',decreases for increasing values of '$\bar{a}$'.

Fig(1.5) shows the variation of film pressure '$\bar{p}$', and different values of k with q=0.1. It is observed that '$\bar{p}$', increasing for increasing values of 'k'.

LOAD CARRYING CAPACITY:

Fig (1.6) shows that the variation of the non-dimensional load carrying capacity '$\overline{W}$' with 'ε' for different values of 'q' at k=0.5. It is observed that the load capacity increase with increasing values of 'ε' and the load capacity decreases for increasing values of 'q'. The corresponding values of load for different 'q' are shown in table (1.1).

Fig (1.7) shows that the variation of the non-dimensional load carrying capacity '$\overline{W}$',with 'q' for different values of 'ε', at k=0.5. It is observed that the load capacity decreases with increasing values of 'q' and the load capacity increases for increasing values of 'ε'. The corresponding values of load at different 'ε',are shown in table (1.2).

Fig (1.8) shows that the variation of the non-dimensional load carrying capacity '$\overline{W}$'with 'q' for different values of 'k' at $\bar{a}$=0.1. It is observed that the load capacity decreases with increasing values of 'q' and the load capacity increases for increasing values of 'k'. The corresponding values of the load '$\overline{W}$' at different 'k' are shown in table (1.3).

Fig(1.9) shows that the variation of the non-dimensional load carrying capacity '$\overline{W}$'with 'q' for different values of '$\bar{a}$'. It is observed that the load capacity decreases with

increasing values of 'q' and the load capacity decreases for increasing values of '$\bar{a}$' at k<1. The corresponding values of the load '$\overline{W}$' at different '$\bar{a}$' are shown in table (1.4).

1.4 GRAPHS:

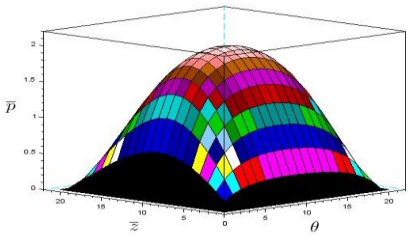

q=0.3, $\overline{p}$ =2.03230127990072

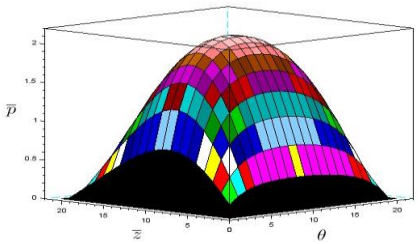

q=0.2, $\overline{p}$ = 2.214355030045597

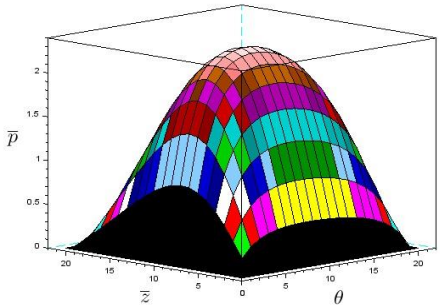

q=0.1, $\bar{p}$ **= 2.355465945596239**

Fig 1.3: The non-Dimensionless pressure ' $\bar{p}$ **'for different values of 'q' with a=0.1, R=1.5,** ε**=0.4, λ=0.7**

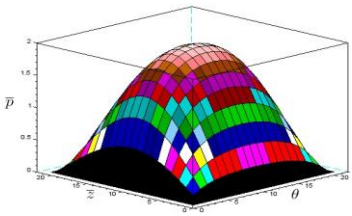

a=0.1, $\bar{p}$ **=1.983636565406811**

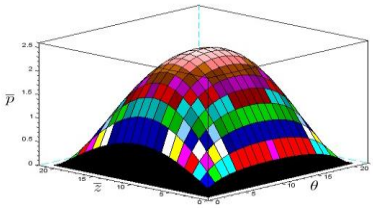

a=0.01, $\bar{p}$ **= 2.455285750254697**

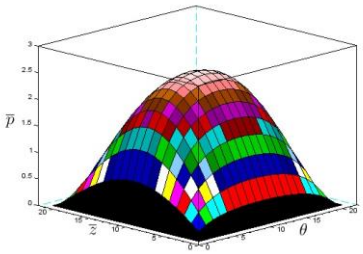

a=0.001, $\bar{p}$ **= 2.522529964714077**

Fig 1.4: The non-Dimensionless pressure ' $\bar{p}$ **'for different values of '**$\bar{a}$**, with k=0.5, q==0.1,** ε**=0.4, λ=0.75**

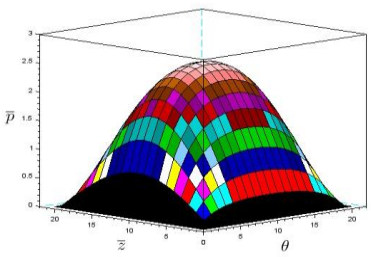

K=1, $\bar{p}$ **= 2.530321510631443**

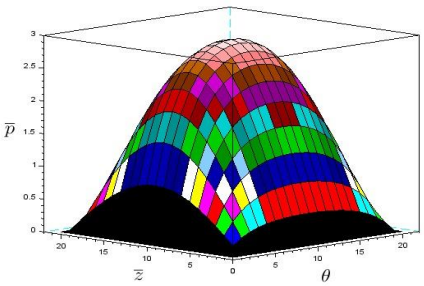

K=2, $\bar{p}$ **= 2.939949783363757**

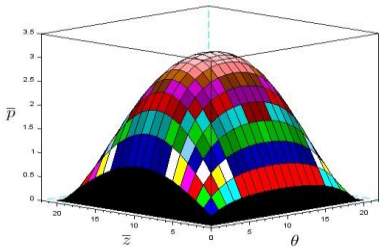

K=3, $\overline{p}$ = 3.109080349522665

Fig 1.5: The non-Dimensionless pressure '$\overline{p}$'for different values of 'k' with $\overline{a}$ =0.1,q==0.1, ε=0.4, λ=0.75

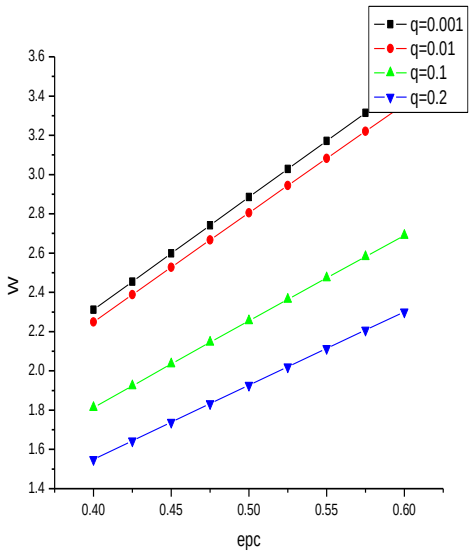

Fig 1.6: The dimensionless load '$\overline{W}$' with 'ε' for different 'q'

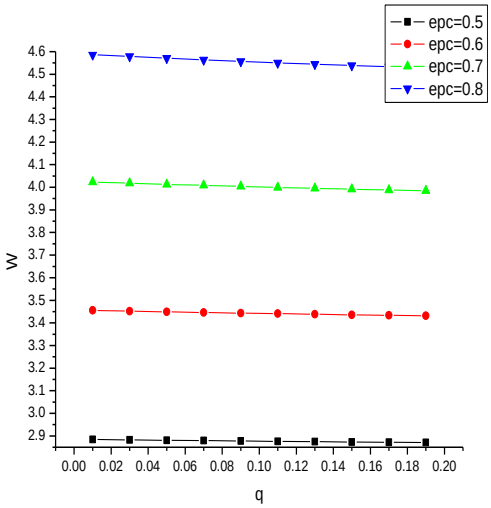

Fig 1.7: Dimensionless load '$\overline{W}$ 'with'q' for different values of 'ε'

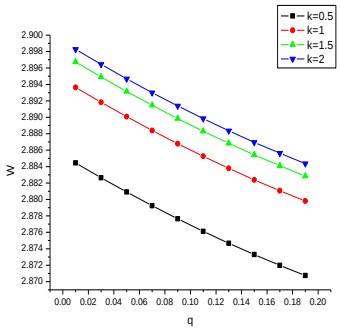

Fig1.8: The dimensionless load '$\overline{W}$' with 'q' for different values of 'k'

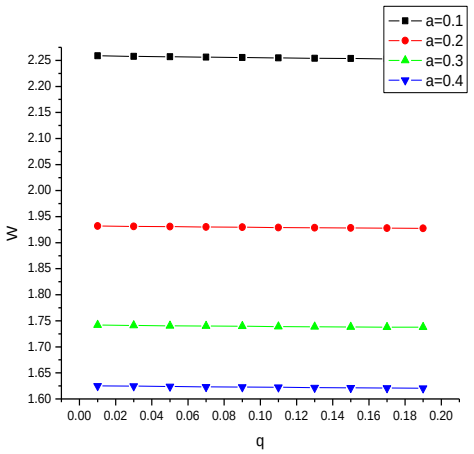

Fig 1.9: The dimensionless load '$\overline{W}$' with 'q' for different values of 'a'

1.5 TABLES:

Table (1.1): The dimensionless load '$\overline{W}$' Vs 'ε' for different 'q'

ε	q=0.001	q=0.01	q=0.1	q=0.2
0.4	2.3112	2.24867	1.81281	1.548982
0.425	2.45493	2.38813	1.924	1.644106
0.45	2.59852	2.52738	2.03478	1.738926
0.475	2.74197	2.66642	2.14515	1.833426
0.5	2.88528	2.80521	2.25506	1.927591
0.525	3.02842	2.94376	2.36449	2.021404
0.55	3.1714	3.08203	2.47341	2.11485
0.575	3.3142	3.22001	2.58179	2.207917
0.6	3.45683	3.35769	2.68959	2.30059

Table (1.2): The dimensionless load '$\overline{W}$' with 'q' for different 'ε'

q	epc=0.5	epc=0.6	epc=0.7	epc=0.8
0.01	2.88444	3.45537	4.02293	4.58642

0.03	2.88264	3.45222	4.01785	4.57862
0.05	2.8809	3.4492	4.01297	4.57115
0.07	2.87924	3.4463	4.0083	4.56401
0.09	2.87765	3.44353	4.00384	4.55718
0.11	2.87613	3.44088	3.99958	4.55067
0.13	2.87468	3.43836	3.99553	4.54448
0.15	2.8733	3.43597	3.99168	4.53861
0.17	2.87198	3.43369	3.98803	4.53305
0.19	2.87074	3.43154	3.98458	4.52779

Table (1.3): The dimensionless load '$\overline{W}$' with 'q' for different 'k'

q	K=0.5	K=1	K=1.5	K=2
0.01	2.88444	2.89365	2.89673	2.89827
0.03	2.88264	2.89182	2.8949	2.89644
0.05	2.8809	2.89008	2.89315	2.89469
0.07	2.87924	2.8884	2.89146	2.893
0.09	2.87765	2.88679	2.88985	2.89138
0.11	2.87613	2.88525	2.88831	2.88984
0.13	2.87468	2.88379	2.88684	2.88836
0.15	2.8733	2.88239	2.88544	2.88696
0.17	2.87198	2.88106	2.8841	2.88563
0.19	2.87074	2.87981	2.88284	2.88436

Table (1.4): The dimensionless load '$\overline{W}$' with 'q' for different '$\overline{a}$'

q	a=0.1	a=0.2	a=0.3	a=0.4
0.01	2.25877	1.93204	1.7417	1.62517
0.03	2.25785	1.93137	1.74109	1.62453

0.05	2.25699	1.93075	1.74052	1.62392
0.07	2.25617	1.93018	1.73999	1.62336
0.09	2.25542	1.92966	1.73951	1.62284
0.11	2.25472	1.92918	1.73906	1.62236
0.13	2.25407	1.92875	1.73866	1.62191
0.15	2.25347	1.92836	1.7383	1.62151
0.17	2.25293	1.92802	1.73798	1.62114
0.19	2.25244	1.92772	1.73771	1.62081

1.6 SUMMARY:

- This paper analyzes the lubrication of Finite journal bearings under operating conditions while taking additive and thermal effects into account.
- Using a grid spacing of $\theta=9^0$and $\bar{\Delta z}$ =0.05., the finite journal bearing with modified Reynolds equation is numerically solved using the finite difference method.For pressure and load capacity, graphs are drawn.
- It has been demonstrated that a high viscous layer near the lubricant's perimeter layer causes an increase in pressure and load capacity, while a low viscous layer causes a drop.
- It is clear that as the thermal impact grows, pressure rises and load capacity falls.

NOMENCLATURE

a	peripheral layer thickness
p	pressures
h	Film thickness
μ	Viscosity of the fluid
x,y,z	Cartesian coordinates
θ	Circumference angle
c	Clearance
e	Eccentricity
R	Radius of the shaft
K	Ratio of viscosity near the surface to the purely hydrodynamic
u, v,w	Velocity component of the film in x,y,z direction

U	Velocity
E	Eccentricity ratio
q	Thermal factor

REFERENCES

1. Peripheral layer thickness Bird, R. B., "Theory of diffusion", In advances in Chemical Engineering, T. B. Drew and J. W. Hoopoes, Jr. (Eds.), Academic Press, N. Y., Vol. 1 (1956), p. 195.
2. Bramhall, A. D., Hutton, J. F., "Wall effect in the flow of lubricating greases in plunger viscometers", Brit. J. App. Phys., Vol. 11 (1960), p. 363.
3. Burgdorfer, A., "The influence of molecular mean free path on the performance of hydrodynamic gas lubricated bearing", J. Bas. Eng. Vol. 81D (1959), p. 94.
4. Cameron, A. "The viscous wedge", Trans. ASME, Vol. 1 (1958), p. 248.
5. Davenport, T. C., "The Rheology of lubricants", Wiley N. Y., Vol. 19 (1973), p. 100.
6. Dowson, D., "A generalized Bramhall, A. D., Hutton, J. F., "Wall effect in the flow of lubricating greases in plunger viscometers", Brit. J. App. Phys., Vol. 11 (1960), p. 363.
7. Hsing, F. C., Malanoski, S. B., "Mean free path effect in spiral – grooved thrust bearing", J. Lub. Tech., Trans. ASME, Vol. 91F (1969), p. 69.
8. Kennard, E. H., "Kinetic theory of gases", McGraw Hill Book Comp., Inc. N. Y., (1938), p. 292.
9. Khonasari, M.M., and Brewe, D., "On the performance of finite journal bearing lubricated with micropolar Fluid", *Trans.Tribol*, Vol. 32 (2), pp. 155-160, 1989.
10. Lamb, H., "Hydrodynamic", Dover, N. Y. (1945), p. 576.
11. Lamb, H., "Hydrodynamic", Dover, N. Y. (1945), p. 576.
12. Murti, P.R.K., "Hydrodynamic lubrication of long porous bearings", *Wear*, Vol. 18, pp. 449- 460, 1971.
13. Naduvinamani, N.B.,andKashinath, B., "Surface roughness effects on the static and dynamic behavior of squeeze film lubrication of short journal bearings with micropolar fluids." *J. Engg. Tribol*, Vol. 222, pp. 1-11, 2008.
14. Prakash, J. and Sinha, P., "Cyclic Squeeze films in micropolar fluid lubricated journal bearings". *Trans. ASME. J. Lubr. Technol*, Vol. 98, pp. 412-417,1975.
15. Reynolds equation for fluid film lubrication", Int. J. Mech. Sci., Vol. 4 (1962), p. 159.

16. Reynolds, O., "On the theory of lubrication and its application to Mr. Beauchamp Tower Experiment", Phil. Roy. Soc. Lon., 177 Part 1 (1886), p.157.

17. Sinha, P., "Dynamically loaded micropolar fluid lubricated journal bearings with special reference to the squeeze films under fluctuating loads", *Wear,* Vol. 45, pp. 279-292,1977.

18. Tseng, R. C., "Rarefaction effects of gas lubricated bearings in a magnetic recording disk file", J. Lub. Tech., Trans. ASME, Vol. 97F (1975), p.624.

19. V.Bharat Kumar, P.Suneetha and Prof.K.R.Prasad, "Effects of additives in finite journal bearings using finite difference method" International Journal of advanced research (2014), Volume 2, Issue 5, 410-425.